

Reversible Anion Exchanges between the Layered Organic–Inorganic Hybridized Architectures: Syntheses and Structures of Manganese(II) and Copper(II) Complexes Containing Novel Tripodal Ligands

Jian Fan,^[a] Lu Gan,^[a] Hiroyuki Kawaguchi,^[b] Wei-Yin Sun,^{*[a]} Kai-Bei Yu,^[c] and Wen-Xia Tang^[a]

Abstract: Six noninterpenetrating organic–inorganic hybridized coordination complexes, $[\text{Mn}(\mathbf{3})_2(\text{H}_2\text{O})_2](\text{ClO}_4)_2 \cdot 2\text{H}_2\text{O}$ (**5**), $[\text{Mn}(\mathbf{3})_2(\text{H}_2\text{O})_2](\text{NO}_3)_2$ (**6**), $[\text{Mn}(\mathbf{3})_2(\text{N}_3)_2] \cdot 2\text{H}_2\text{O}$ (**7**), $[\text{Cu}(\mathbf{3})_2(\text{H}_2\text{O})_2](\text{ClO}_4)_2$ (**8**), $[\text{Mn}(\mathbf{4})_2(\text{H}_2\text{O})(\text{SO}_4)] \cdot \text{CH}_3\text{OH} \cdot 5\text{H}_2\text{O}$ (**9**) and $[\text{Mn}(\mathbf{4})_2](\text{ClO}_4)_2$ (**10**) were obtained through self-assembly of novel tripodal ligands, 1,3,5-tris(1-imidazolyl)benzene (**3**) and 1,3-bis(1-imidazolyl)-5-(imidazol-1-ylmethyl)benzene (**4**) with the corresponding metal salts, respectively. Their structures were determined by X-ray crystallography. The results of

structural analysis of complexes **5**, **6**, **7**, and **8** with rigid ligand **3** indicate that their structures are mainly dependant on the nature of the organic ligand and geometric need of the metal ions, but not influenced greatly by the anions and metal ions. While in complexes **9** and **10**, which contain the flexible ligand **4**, the counteranion plays an important role in

the formation of the frameworks. Entirely different structures of complexes **5** and **10** indicate that the organic ligands greatly affect the structures of assemblies. Furthermore, in complexes **5** and **6**, the counteranions located between the cationic layers can be exchanged by other anions. Reversible anion exchanges between complexes **5** and **6** without destruction of the frameworks demonstrate that **5** and **6** can act as cationic layered materials for anion exchange, as determined by IR spectroscopy, elemental analyses, and X-ray powder diffraction.

Keywords: anion exchange · organic–inorganic hybrid composites · self-assembly · supramolecular chemistry · tripodal ligands

Introduction

In recent years, the most attractive areas of research in the fields of crystal engineering and supramolecular chemistry have been aimed at creating a wide range of purpose-built materials with specific structures and useful properties, such as electronic, magnetic, optical and catalytic properties.^[1–5] A great number of one-dimensional (1D), two-dimensional (2D), and three-dimensional (3D) frameworks have been obtained by assembly of metal salts with rationally designed

organic ligands. For example, a tripodal ligand with an arene core, 1,3,5-tris(3,5-pyrimidyl)benzene, was treated with $[\text{Pd}(\text{en})(\text{NO}_3)_2]$ (en = ethylenediamine) to give a nanometer-sized hexahedral coordination capsule.^[6] The key step for design and synthesis of supramolecular transition-metal complexes is to select suitable multidentate bridging ligands.^[7] Accordingly, tripodal ligands with N donors are a good choice for the construction of such complexes, especially with arene core-based tripodal ligands.^[8]

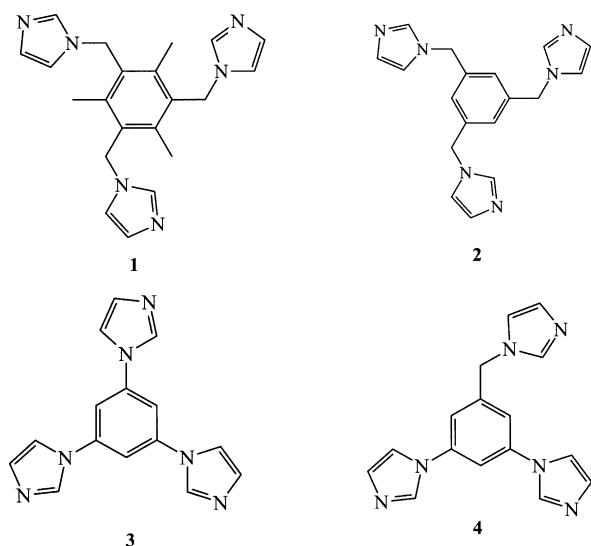
In our previous studies, we reported two tripodal ligands, 1,3,5-tris(imidazol-1-ylmethyl)-2,4,6-trimethylbenzene (**1**) and 1,3,5-tris(imidazol-1-ylmethyl)benzene (**2**, Scheme 1). We demonstrated that they can form individual molecular cages with selective encapsulation of organic compounds, such as camphor, or with anion-exchange properties.^[9] A polymeric coordination complex with a 2D honeycomb structure was obtained by assembly of **1** with copper(II) acetate.^[9d] The results demonstrate that such tripodal ligands are versatile and can adopt different conformations when they interact with metal salts as a consequence of their flexibility since there is a methylene group between the central benzene ring and terminal imidazole group. At the same time, the results also show the complexity of the assembly process of metal salts with such flexible ligands. At present, the self-

[a] Prof. Dr. W.-Y. Sun, J. Fan, L. Gan, Prof. W.-X. Tang
Coordination Chemistry Institute, State Key Laboratory of Coordination Chemistry
Nanjing University, Nanjing 210093 (China)
Fax: (+86)25-331-4502
E-mail: sunwy@nju.edu.cn

[b] Dr. H. Kawaguchi
Coordination Chemistry Laboratories
Institute for Molecular Science, Myodaiji, Okazaki 444-8585 (Japan)

[c] Prof. K.-B. Yu
Analysis Center
Chengdu Branch of Chinese Academy of Science, Chengdu 610041 (China)

Supporting information for this article is available on the WWW under <http://www.chemeurj.org> or from the author.

Scheme 1. Tripodal ligands **1–4**.

assembly process depends on many and/or even subtle factors and is often difficult to predict exactly.^[10] This encouraged us to undertake further studies on analogues/derivatives of **1** and **2** as organic ligands, which may lead to a great variety of structures. Following this approach, we now expand this system with another two novel tripodal ligands, 1,3,5-tris(1-imidazolyl)benzene (**3**) and 1,3-bis(1-imidazolyl)-5-(1-methylimidazol-1-yl)methyl)benzene (**4**, Scheme 1). Six noninterpenetrating organic–inorganic hybridized coordination complexes, $[\text{Mn}(\mathbf{3})_2(\text{H}_2\text{O})_2](\text{ClO}_4)_2 \cdot 2\text{H}_2\text{O}$ (**5**), $[\text{Mn}(\mathbf{3})_2(\text{H}_2\text{O})_2](\text{NO}_3)_2$ (**6**), $[\text{Mn}(\mathbf{3})_2(\text{N}_3)_2] \cdot 2\text{H}_2\text{O}$ (**7**), $[\text{Cu}(\mathbf{3})_2(\text{H}_2\text{O})_2](\text{ClO}_4)_2$ (**8**), $[\text{Mn}(\mathbf{4})_2(\text{H}_2\text{O})(\text{SO}_4)] \cdot \text{CH}_3\text{OH} \cdot 5\text{H}_2\text{O}$ (**9**), and $[\text{Mn}(\mathbf{4})_2](\text{ClO}_4)_2$ (**10**) were successfully isolated.

Supramolecular architectures have attracted much attention not only because of their fantastic structures, but also because of their potential applications, such as ion and molecular recognition, and ion-exchange.^[9a, 11–12] Yaghi and co-workers have reported a metal–organic framework con-

taining large rectangular channels that was obtained by self-assembly of $\text{Cu}(\text{NO}_3)_2 \cdot 2.5\text{H}_2\text{O}$ with 4,4'-bipyridine. In this complex, most of the nitrate ions can be exchanged by SO_4^{2-} and BF_4^- .^[12a] However, no reversible anion exchange of the layered materials with an open framework was reported to now, although a cationic layered material for anion-exchange was reported by Oliver very recently.^[11] Here, we present the reversible anion-exchange behavior of complexes **5** and **6**.

Results and Discussion

X-ray diffraction studies: To investigate the influence of the counteranions on the formation of the frameworks, we carried out reactions between the ligand **3** and manganese(II) salts with various anions and succeeded in isolating three manganese(II) complexes, $[\text{Mn}(\mathbf{3})_2(\text{H}_2\text{O})_2](\text{ClO}_4)_2 \cdot 2\text{H}_2\text{O}$ (**5**), $[\text{Mn}(\mathbf{3})_2(\text{H}_2\text{O})_2](\text{NO}_3)_2$ (**6**) and $[\text{Mn}(\mathbf{3})_2(\text{N}_3)_2] \cdot 2\text{H}_2\text{O}$ (**7**). The complexes **5–7** were synthesized by a layering method and were found to be insoluble in water and common organic solvents, such as methanol, acetonitrile, and acetone. Their structures were determined by X-ray crystallography. Similar cell parameters of complexes **5–7** (Table 1) indicate that they are isomorphous and isostructural. Thus, as a typical example, the structure of complex **5** is described in detail.

The crystal structure of complex **5** (cationic part) is shown in Figure 1 a. Each manganese(II) atom has a slightly distorted octahedral coordination environment with four imidazole N atoms from four different **3** ligands and two O atoms from two water molecules. The coordination angles vary between $87.11(10)$ and 180° and Mn–O1, Mn–N1, and Mn–N4D bond lengths are 2.180(2), 2.249(3), and 2.253(2) Å, respectively (Table 2). Two coordinated water molecules lie in the opposite direction with respect to the manganese(II) atoms. Note that in complex **7** the coordinated water molecules are replaced by azide anions and the complex is neutral with one manganese(II) atom and two azide anions. Interestingly, each ligand **3** coordinates to two manganese(II) atoms as a

Table 1. Summary of crystal data and refinement results for complexes **5–10**.

Compound	5	6	7	8	9	10
formula	$\text{C}_{30}\text{H}_{32}\text{Cl}_2\text{MnN}_{12}\text{O}_{12}$	$\text{C}_{30}\text{H}_{28}\text{N}_{14}\text{MnO}_8$	$\text{C}_{30}\text{H}_{28}\text{MnN}_{18}\text{O}_2$	$\text{C}_{30}\text{H}_{28}\text{CuCl}_2\text{N}_{12}\text{O}_{10}$	$\text{C}_{33}\text{H}_{44}\text{N}_{12}\text{MnO}_{11}\text{S}$	$\text{C}_{32}\text{H}_{28}\text{Cl}_2\text{N}_{12}\text{MnO}_8$
formula weight	878.49	767.58	727.64	823.11	859.77	834.49
crystal system	monoclinic	monoclinic	monoclinic	monoclinic	triclinic	monoclinic
space group	$P2_1/n$	$P2_1/n$	$P2_1/n$	$P2_1/c$	$\bar{P}1$	Cc
a [Å]	9.233(1)	10.626(5)	10.056(1)	9.826(9)	12.542(6)	12.116(6)
b [Å]	11.613(2)	11.599(5)	12.280(2)	10.891(9)	12.942(5)	17.728(8)
c [Å]	17.989(3)	13.583(6)	13.665(2)	17.11(1)	13.708(6)	17.415(8)
α [°]					65.00(2)	
β [°]	90.63(1)	111.114(7)	108.56(1)	106.61(1)	80.33(3)	96.068(7)
γ [°]					66.23(2)	
V [Å ³]	1928.7(5)	1561.7(11)	1599.7(4)	1754.7(23)	1845(1)	3719(3)
Z	2	2	2	2	2	4
μ [mm ⁻¹]	0.552	0.501	0.475	0.843	0.488	0.564
reflections collected	3961	12383	3243	13714	14703	14575
observed reflections	2626	2734	2291	4033	4815	3649
R_1		0.0370		0.0340	0.1030	0.0550
R_w		0.0850		0.0890	0.2850	0.1450
$R_1 [I > 2\sigma(I)]$	0.0543		0.0293			
$wR_2 [I > 2\sigma(I)]$	0.1636		0.0710			

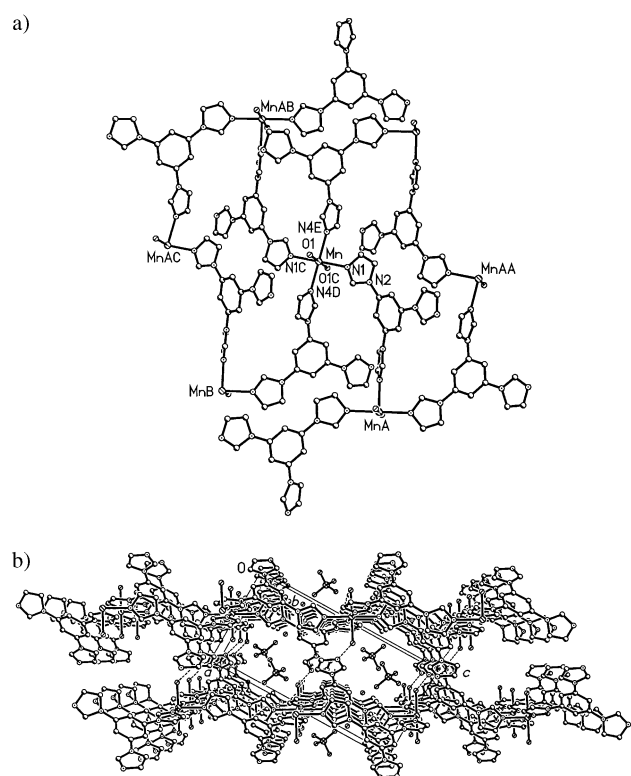


Figure 1. a) The 2D network structure of compound **5** viewed from above. b) Crystal packing diagram of **5** on *ac* plane.

bidentate ligand rather than a tridentate ligand that connects three metal atoms. Such a coordination mode means that complex **5** forms an infinite 2D network structure. Four manganese(II) atoms (i.e. Mn, MnB, MnAC, and MnAB in Figure 1a) and four molecules of **3** ligand form a 40-membered ring. Thus the framework of complex **5** can be regarded as a (4,4) network. All the manganese(II) atoms in one layer of **5** are in the same plane, and the benzene ring planes of **3** are greatly deflected from the manganese(II) plane with a dihedral angle of 41.6°.

In complex **5**, the uncoordinated N atom of the imidazole in ligand **3** forms a O–H⋯N hydrogen bond with coordinated water molecule from the adjacent layer to link the 2D networks to generate a 3D framework (Figure 1b). The hydrogen bond lengths and angles are summarized in Table 3. The perchlorate anions occupy the voids created between the 2D layers and are bound to the framework through (water) O–H⋯O (perchlorate) and C–H⋯O (perchlorate) hydrogen bonds (Table 3). Similar crystal packing was found in the complex of **6** (Figure S1 in the Supporting Information), in which the uncoordinated nitrate anions are also located in the voids between two 2D layers, and complex **7** (Figure S2 in the Supporting Information). A crystallographic study reveals that the structures of complexes **5–7** are very similar with regard to the coordination mode, network structure, and crystal packing. This fact indicates that the structures of the assemblies mainly depend on the nature of the organic ligand

Table 2. Selected bond lengths [Å] and angles [°] for complexes **5–10**.

[Mn(3) ₂ (H ₂ O) ₂](ClO ₄) ₂ · 2H ₂ O (5)					
Mn–O1	2.180(2)	Mn–N1	2.249(3)	Mn–N4A	2.253(2)
O1–Mn–N1B	92.89(10)	O1–Mn–N1	87.11(10)	O1–Mn–N4A	89.11(10)
O1b–Mn–N4A	90.89(10)	N1–Mn–N4A	89.36(9)	N1b–Mn–N4A	90.64(9)
[Mn(3) ₂ (H ₂ O) ₂](NO ₃) ₂ (6)					
Mn1–O1	2.2192(17)	Mn1–N1	2.2335(17)	Mn–N5C	2.2446(16)
O1–Mn1–N1	91.84(6)	O1–Mn1–N1D	88.16(6)	O1–Mn–N5C	91.93(6)
O1d–Mn–N5C	88.07(6)	N1–Mn–N5C	89.78(6)	N1d–Mn–N5C	90.22(6)
[Mn(3) ₂ (N ₃) ₂] · 2H ₂ O (7)					
Mn–N1	2.2442(15)	Mn–N4E	2.2571(14)	Mn–N7	2.2639(17)
N1–Mn–N4F	89.91(5)	N1–Mn–N4E	90.09(5)	N1–Mn–N7G	88.59(6)
N1–Mn–N7	91.41(6)	N4E–Mn–N7	92.10(6)	N4F–Mn–N7	87.90(6)
[Cu(3) ₂ (H ₂ O) ₂](ClO ₄) ₂ (8)					
Cu1–O1	2.430(2)	Cu1–N1	2.021(2)	Cu1–N3H	2.007(2)
O1–Cu1–N1	89.55(12)	O1–Cu–N1I	90.45(12)	O1–Cu–N3H	91.17(12)
O1I–Cu–N3H	88.83(12)	N1–Cu–N3H	90.90(12)	N1i–Cu–N3H	89.10(12)
[Mn(4) ₂ (H ₂ O)(SO ₄)] · CH ₃ OH · 5H ₂ O (9)					
Mn1–O1	2.184(5)	Mn1–N1	2.284(6)	Mn1–N9	2.229(6)
Mn2–O5	2.215(4)	Mn2–N3	2.250(6)	Mn2–N7	2.255(6)
O1–Mn1–N9J	94.2(2)	O1–Mn1–N1	90.5(2)	O1–Mn1–N1J	89.5(2)
O1–Mn1–N9	85.8(2)	N1–Mn1–N9	87.1(2)	N1–Mn1–N9J	92.9(2)
O5–Mn2–N3	92.4(2)	O5–Mn2–N3K	87.6(2)	O5–Mn2–N7	90.0(2)
O5–Mn2–N7K	90.0(2)	N3–Mn2–N7	93.8(2)	N3–Mn2–N7K	86.2(2)
[Mn(4) ₂](ClO ₄) ₂ (10)					
Mn1–N1	2.243(5)	Mn1–N7	2.246(5)	Mn1–N3L	2.285(5)
Mn1–N5M	2.260(5)	Mn1–N9N	2.266(5)	Mn1–N11O	2.314(5)
N1–Mn1–N3L	98.4(2)	N1–Mn1–N5M	84.4(2)	N1–Mn1–N7	178.7(2)
N1–Mn1–N9N	96.2(2)	N3L–Mn1–N5M	84.0(2)	N3L–Mn1–N7	82.5(2)
N3L–Mn1–N9N	93.3(2)	N5M–Mn1–N7	94.4(2)	N7–Mn1–N9N	85.1(2)
N5M–Mn1–N9N	177.3(2)				

Symmetry transformations used to generate equivalent atoms: A) $x - \frac{1}{2}, \frac{1}{2} - y, z + \frac{1}{2}$; B) $-x, -y, 1 - z$; C) $3/2, y - \frac{1}{2}, -z - \frac{1}{2}$; D) $3/2 - x, 5/2 + x, \frac{1}{2} - z$; E) $-x + \frac{1}{2}, y - \frac{1}{2}, \frac{1}{2} + z$; F) $x - \frac{1}{2}, \frac{1}{2} - y, \frac{1}{2} + z$; G) $-x, -y, 1 - z$; H) $x, -y + 3/2, z - \frac{1}{2}$; I) $2 - x, 1 - y, z$; J) $1 - x, 4 - y, -1 - z$; K) $2 - x, 2 - y, z$; L) $-1 + x, -\frac{1}{2} + y, z$; M) $-1 + x, y, \frac{1}{2} + x$; N) $x, -y, -\frac{1}{2} + z$; O) $x + 1, y, z$.

Table 3. Distances [Å] and angles [°] of hydrogen bonding between donors (D) and acceptors (A) for complexes **5–10**.^[a]

D–H...A ^[b]	Distance (D...A)	D–H–A	Angle (D–H–A)
[Mn(3)₂(H₂O)₂](ClO₄)₂·2H₂O (5)			
C5–H5...O2A	3.254(8)	C5–H5...O2A	149
C7–H7...O2B	3.488(9)	C7–H7...O2B	173
C2–H2...O3	3.405(9)	C2–H2...O3	163
C13–H13...O3	3.490(10)	C13–H13...O3	172
O1–H1A...O5C	2.939(7)	O1–H1A...O5C	162
O1–H1B...M6D	2.742(4)	O1–H1B...M6D	171
[Mn(3)₂(H₂O)₂](NO₃)₂ (6)			
O1–H13...O4E	2.784(3)	O1–H13...O4E	169
O1–H14...O3F	2.924(3)	O1–H14...O3F	175
C6–H6...O3G	3.180(4)	C6–H6...O3G	150
C4–H4...O2	3.346(3)	C4–H4...O2	163
C13–H11...O2	3.375(3)	C13–H11...O2	167
C15–H12...O2H	3.501(3)	C15–H12...O2H	158
C1–H1...M3E	3.450(4)	C1–H1...M3E	144
[Mn(3)₂(N₃)₂]·2H₂O (7)			
O–H0A...M9I	2.898(3)	O–H0A...M9I	172
O–H0B...M7	3.014(3)	O–H0B...M7	168
C12–H12...OJ	3.325(3)	C12–H12...OJ	143
C15–H15...OJ	3.496(3)	C15–H15...OJ	164
[Cu(3)₂(H₂O)₂](ClO₄)₂ (8)			
O1–H14...O5K	3.025(4)	O1–H14...O5K	158
C1–H1...O4K	3.451(5)	C1–H1...O4K	162
C6–H6...O2L	3.380(4)	C6–H6...O2L	164
C8–H8...O4M	3.351(5)	C8–H8...O4M	141
C15–H12...O3N	3.373(4)	C15–H12...O3N	142
O1–H13...M5O	2.780(4)	O1–H13...M5O	170
[Mn(4)₂(H₂O)(SO₄)]·CH₃OH·5H₂O (9)			
C1–H1...O3P	3.209(10)	C1–H1...O3P	168
C5–H6...O3Q	3.193(8)	C5–H6...O3Q	157
C10–H11...O3Q	3.479(8)	C10–H11...O3Q	171
C14–H13...O3Q	3.493(8)	C14–H13...O3Q	169
C20–H20...O4P	3.223(10)	C20–H20...O4P	154
C25–H25...O4P	3.408(10)	C25–H25...O4P	167
C30–H27...O4P	3.404(9)	C30–H27...O4P	157
C2–H2...O11	3.358(15)	C2–H2...O11	140
C18–H16...O6R	3.461(10)	C18–H16...O6R	161
C26–H18...O9	3.102(15)	C26–H18...O9	162
C22–H22...O8	3.291(13)	C22–H22...O8	163
C23–H23...O6S	3.453(11)	C23–H23...O6S	173
C32–H28...O6S	3.461(12)	C32–H28...O6S	167
O2A...O11A ^[b]	2.78		
O11A...O8B ^[b]	2.68		
O8B...O7B ^[b]	2.72		
O7B...O5B ^[b]	2.71		
O5B...O2A ^[b]	2.68		
[Mn(4)₂](ClO₄)₂ (10)			
C2–H2...O5 α	3.459(11)	C2–H2...O5 α	178
C5–H6...O5 β	3.483(11)	C5–H6...O5 β	169
C10–H11...O3 γ	3.438(10)	C10–H11...O3 γ	153
C14–H13...O4 β	3.428(11)	C14–H13...O4 β	151
C17–H15...O1 α	3.388(11)	C17–H15...O1 α	158
C19–H17...O10 δ	3.30(5)	C19–H17...O10 δ	168
C20–H19...O5 δ	3.460(10)	C20–H19...O5 δ	154
C23–H22...O6 δ	3.40(2)	C23–H22...O6 δ	165
C30–H27...O4 ϵ	3.462(12)	C30–H27...O4 ϵ	154

[a] Symmetry transformation used to generate equivalent atoms: A) $-x, 1-y, 1-z$; B) $\frac{1}{2}+x, \frac{3}{2}-y, -\frac{1}{2}+z$; C) $x, -1+y, z$; D) $1-x, 1-y, 1-z$; E) $2-x, 3-y, -z$; F) $-\frac{1}{2}+x, \frac{5}{2}-y, \frac{1}{2}+z$; G) $-\frac{1}{2}+x, \frac{7}{2}-y, \frac{1}{2}+z$; H) $\frac{3}{2}-x, -\frac{1}{2}+y, -\frac{1}{2}-z$; I) $\frac{1}{2}-x, -\frac{1}{2}+y, \frac{3}{2}-z$; J) $\frac{1}{2}+x, \frac{1}{2}-y, -\frac{1}{2}+z$; K) $1-x, \frac{1}{2}+y, \frac{1}{2}-z$; L) $1+x, \frac{1}{2}-y, \frac{1}{2}+z$; M) $2-x, -y, 1-z$; N) $1+x, y, z$; O) $-1+x, \frac{1}{2}-y, -\frac{1}{2}+z$; P) $1-x, 4-y, -1-z$; Q) $x, -1+y, 1+z$; R) $2-x, 2-y, -z$; S) $-1+x, y, z$; a) $-\frac{1}{2}+x, -\frac{1}{2}+y, z$; β) $\frac{1}{2}+x, -\frac{1}{2}+y, z$; γ) $x, -y, -\frac{1}{2}+z$; δ) $-\frac{1}{2}+x, \frac{1}{2}-y, \frac{1}{2}+z$; e) $-1+x, y, z$. [b] For atom numbering see Figure 3b.

and geometric requirements of the metal ions, but are not greatly influenced by the anions in this system.

One of the unique features concerning the crystal engineering of organic–inorganic hybridized compounds is that the role of metal atoms can be evaluated.^[13] Here, we have a good opportunity to compare the role of the metal ions in the self-assembly of complexes of **3** with different metal ions, namely [Mn(**3**)₂(H₂O)₂](ClO₄)₂·2H₂O (**5**) and [Cu(**3**)₂(H₂O)₂](ClO₄)₂ (**8**). Compound **8** was synthesized by a hydrothermal method by reaction of Cu(ClO₄)₂·6H₂O with ligand **3**. The coordination environment around the copper(II) atom consists of four short in-plane Cu–N (Cu1–N1 = Cu1–N1C = 2.021(2), Cu1–N3D = Cu1–N3E = 2.007(2) Å) bonds and the two long axial Cu–O (Cu1–O1 = Cu1–O1C = 2.430(2) Å) bonds as shown in Figure 2a. The manganese(II) atom in **5** and the copper(II) atom in **8** are both six-coordinate and each **3** acts as a bidentate ligand in complexes **5** and **8** to connect two metal atoms to give 2D networks. The rigidity of ligand **3** and the six-coordinate metal ions may be responsible for the similarity of the structures **5–8**. However, there is an apparent difference between complexes **5** and **8**. In complex **8**, the plane formed by four N atoms coordinated to one copper(II) atom are not in the plane formed by the copper(II) atoms, for example, the dihedral angle between the plane through N1, N3D, N1C, N3E (Figure 2a) and that formed by copper(II) is 41.7°, while in the case of **5**, the corresponding dihedral angle of 8.2° means that the plane of four N atoms (i.e. N1, N4D, N1C, and N4E in Figure 1a) coordinated to one manganese(II) atom are almost in the same plane as that formed by the manganese(II) atoms. In addition, as illustrated in Figure 2b, 2D sheets of **8** are connected by O–H...N hydrogen bonds to give a 3D framework which is same as **5**. However, the perchlorate anions in **8** occupy the vacancies in 2D network rather than the voids formed between two 2D layers, as observed in **5** (Figure 1b).

In contrast to the rigid ligand **3**, ligand **4** has a pendant arm owing to a methylene group between the central benzene ring and terminal imidazole group. The flexibility of **4** may lead to a great variety of structures when it interacts with metal salts. An unexpected coordination polymer **9** with a 1D hinged chain structure was obtained by reaction of ligand **4** with MnSO₄·H₂O. As shown in Figure 3a, the Mn1 atom is coordinated by two O atoms from two sulfate anions and four N atoms of imidazole from four **4**, while the Mn2 atom is coordinated by two water molecules instead of sulfate anions in addition to four N atoms of imidazole groups. Each ligand **4** links two metal atoms using two of three imidazole groups and the third one (i.e. N5, N11 in Figure 3a) is again free of coordination. Two 1D chains are further linked by hydrogen bonds (Table 3) and π – π interactions, as exhibited in Figure 3b. Interestingly, there are five-membered rings between the two adjacent chains formed by five O atoms (i.e. O2A, O5B, O7B, O8B and O11A in Figure 3b) from the coordinated sulfate anion of one chain, the coordinated water molecule of the adjacent chain, solvate water and methanol molecules. The distances, which range from 2.68 to 2.78 Å between each two adjacent O atoms within the five-membered ring, indicate the formation of O–H...O hydrogen bonds (Table 3). A more exciting structural feature of **9** is the

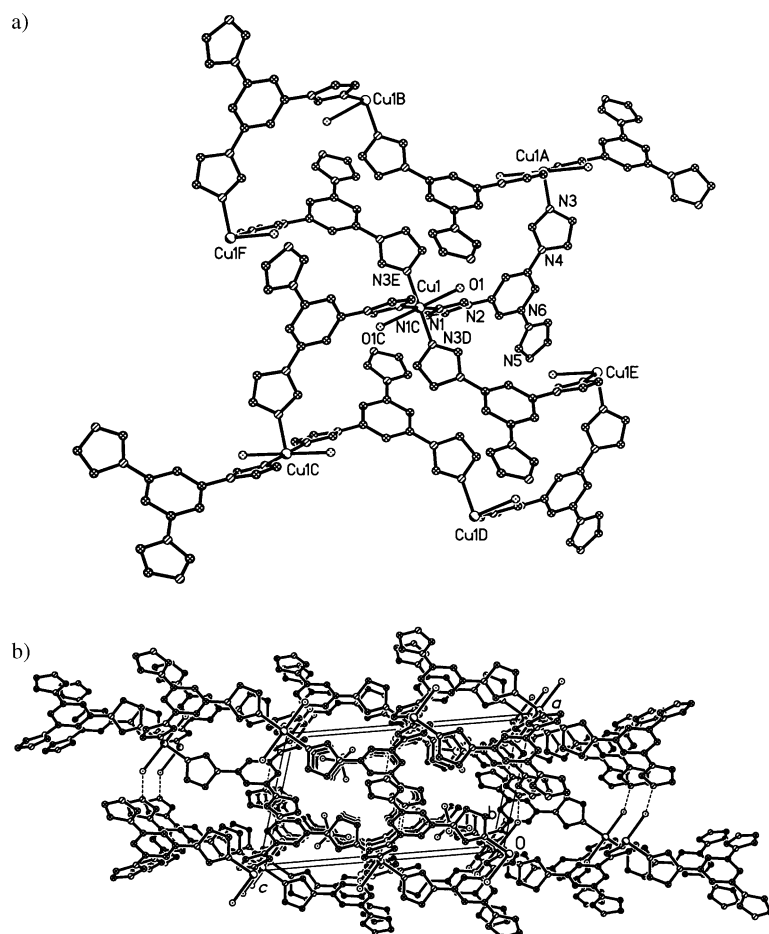


Figure 2. a) 2D network structure of complex 8. b) Crystal packing of 8 on the *ac* plane.

intercalation of the central benzene ring plane together with the uncoordinated imidazole group of ligand 4 in one chain into the adjacent hinged chain, which can be seen more clearly from the space-filling diagram shown in Figure 3c, through the π – π interactions. The nearest centroid–centroid distances between two benzene ring planes and between the benzene ring and the uncoordinated imidazole ring planes are 4.42 and 3.47 Å, respectively, which confirm the existence of π – π interactions.

When $\text{Mn}(\text{ClO}_4)_2 \cdot 6\text{H}_2\text{O}$ was used instead of $\text{MnSO}_4 \cdot \text{H}_2\text{O}$ to react with ligand 4, a novel complex 10 with a 2D network structure, rather than a 1D chain like 9, was obtained. In complex 10, each manganese(II) atom is coordinated by six imidazole N atoms from six different ligands of 4 (Figure 4a). The local coordination environment around the manganese(II) atom can be regarded as a slightly distorted octahedron with Mn–N bond lengths ranging from 2.243(5) to 2.314(5) Å and N–Mn–N bond angles varying from 84.0(2) to 178.7(2)° (Table 2), which are similar to those of other reported manganese(II) complexes.^[14] It is noteworthy that each ligand 4 connects three manganese(II) atoms to give an unprecedented 2D network structure (Figure 4a). Here, 4 acts as a tridentate ligand in complex 10, although 4 in 9 and 3 in 5–8 all act as bidentate ligands. In the reported 2D coordination polymers with network structures, rigid tripodal ligands, for example, 1,3,5-tricyanobenzene and benzene-1,3,5-tricarboxy-

late enclosing an angle of 120°, were used to link the linear metal centers.^[15] In our case, ligand 4, which has a flexible arm, links three six-coordinate metal centers and leads to the formation of a 2D network with double sheets (Figure 4b, c). The perchlorate ions located in the voids of the network (Figure S3 in the Supporting Information) are held there by hydrogen bonds (Table 3).

Complexes 9 and 10, which contain the same ligand and metal atoms but have different network structures, provide nice examples of the significant effect that the counterions have on the construction of organic–inorganic hybridized architectures in a system with a flexible ligand. While in the system with the rigid ligand 3, the anions did not greatly affect the assembly products (*vide supra*). In ligand 4, the flexible arm can coordinate to the metal atom in a position that is well away from the central benzene ring plane. In complexes 9 and 10, the imidazolyl group attached to the flexible arm is essentially perpendicular to the benzene ring plane (dihedral angles of 72.4 and 79.1° in 9, and 77.3 and 79.0° in 10), which endows ligand 4 with the capability of coordinating to metal centers to result in a hinged 1D chain and a 2D network with double sheets. In conclusion, the present study provides evidence that flexible organic ligands may lead to the formation of a great variety of supramolecular frameworks.

Anion-exchange properties of complexes 5 and 6: As revealed by the crystal structures of 5 and 6, the anions were located within the open structures between the cationic layers through hydrogen bonds (Figure 1b and Figure S1 in the Supporting Information). Since both complexes 5 and 6 are not soluble in common solvents, these cationic layered compounds are expected to display anion-exchange properties. Excess NaClO_4 was added to a suspension of well-ground complex 6 in water at room temperature. The mixture was stirred for 24 h to allow anion exchange, then it was filtered, and washed with water several times. The FT-IR spectra of the exchanged solid and the original 6 are shown in Figure 5a and 5d, respectively. Intense bands from $\nu = 1112$ to 1091 cm^{-1} , which originate from the ClO_4^- ion, appeared, while the intense bands from 1384 to 1356 cm^{-1} of the NO_3^- ion disappeared in the spectrum of exchanged solid (Figure 5a). Furthermore, the FT-IR spectrum of the exchanged solid is indistinguishable from that of the as-synthesized complex with the ClO_4^- ion,

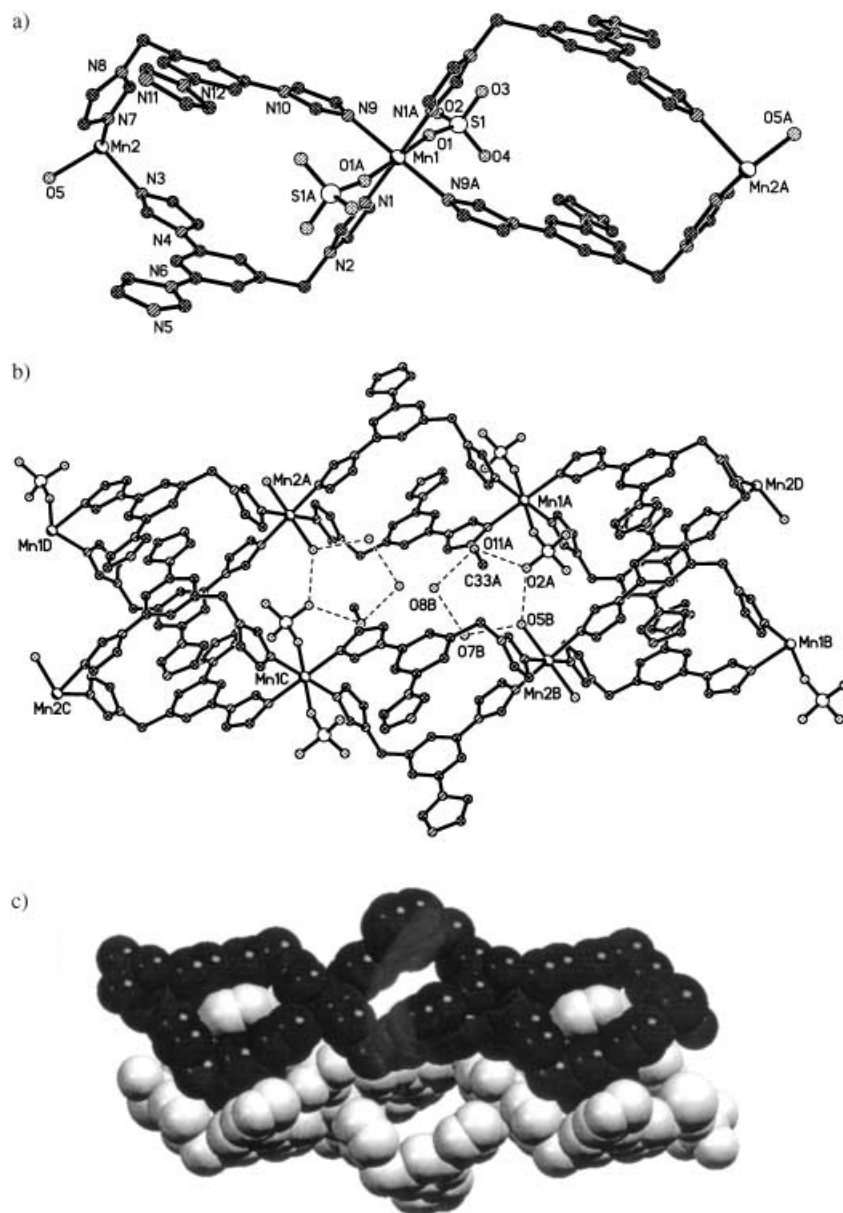


Figure 3. a) 1D chain structure of complex **9**. b) Two 1D chains of **9** linked by hydrogen bonds and π - π interactions. c) Space-filling diagram for two interacting 1D chains of **9**.

namely **5** (Figure 5b). To investigate the reversibility of such anion exchange processes in more detail, the exchanged solid was suspended in an aqueous solution of NaNO_3 with stirring to allow anion exchange again. The ClO_4^- bands disappeared and the NO_3^- bands appeared in the FT-IR spectrum of the obtained solid (Figure 5c), which is almost the same as the spectrum of the original material **6** (Figure 5d). The anion-exchange reactions were also monitored by X-ray powder diffraction techniques. When complex **6** was exchanged with NaClO_4 , the characteristic peaks were different from those of original **6** (Figure 6a and 6d); however, it gives an X-ray powder diffraction pattern similar to that of complex **5** (Figure 6b). The slight shift and broadening of some peaks may be attributed to incomplete recovery of the symmetry of the structure.^[12b, 16] When NaNO_3 was added to the suspension of the exchanged solid in water, the characteristic peaks of

complex **6** reappeared (Figure 6c). The results confirm that reversible anion exchange occurs between the complexes **5** and **6** without the destruction of the frameworks. The anion-exchanged products are also evidenced by elemental analyses (see the Experimental Section).

It is important to prove that such anion exchanges occur by means of a solid-state or a solvent-mediated process.^[17] First, NMR experiments were carried out to check whether any of the ligand is dissolved in the mother liquors after the exchange. Excess Na_2S or NaOH were added to the mother liquor to precipitate any possible manganese(II) ions and to exclude the paramagnetic influence of the manganese(II) ion on the NMR spectrum. The mother liquor was then extracted by CDCl_3 . No signals of the ligand were detected in the CDCl_3 solution, which implies that the amount of dissolved ligand in the mother liquor is too low to be detected by NMR

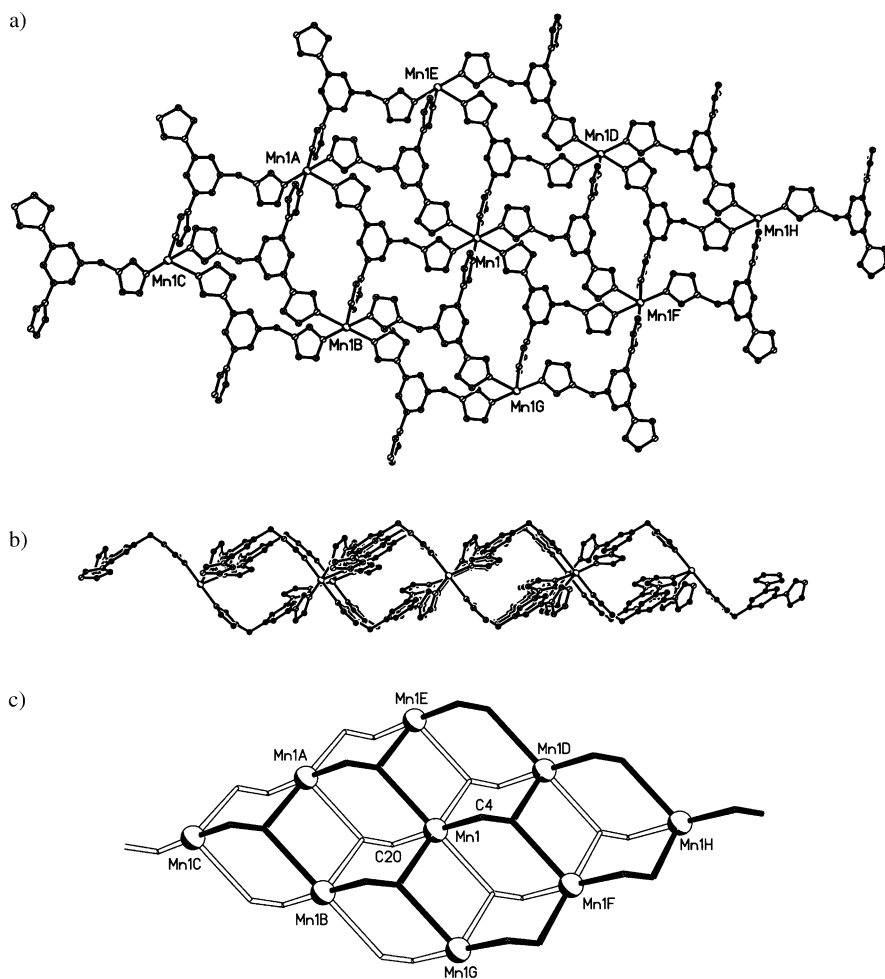


Figure 4. a) Top view and b) side views of the 2D cationic network structure of complex **10**. c) Schematic drawing of 2D network in which ligand **4** is represented by three spokes radiating from the centroid of benzene ring to the Mn centers directly or through the methylene carbon atom (e.g. C4, C20). The solid lines represent the bonds up the plane formed by manganese atoms and open lines down the plane.

spectroscopy. To determine the solubility of the complex in aqueous solutions under exchange conditions, the concentration of manganese(II) ion in the mother liquors after the exchange was measured by atomic absorption spectroscopy. The results show that the concentration of the manganese(II) ion is $<0.01 \text{ mmol L}^{-1}$. Most importantly, the solubility of $[\text{Mn}(\mathbf{3})_2(\text{H}_2\text{O})_2](\text{ClO}_4)_2$ and $[\text{Mn}(\mathbf{3})_2(\text{H}_2\text{O})_2](\text{NO}_3)_2$ in $0.1 \text{ g mL}^{-1} \text{ NaNO}_3$ (concentration used in the anion exchange) aqueous solution are 0.0045 and $0.0096 \text{ mmol L}^{-1}$, respectively. This means that the solubility of the exchanged product is larger than that of the original complex. While the solvent-mediated transformation always occurs from a more soluble species to a less soluble species.^[17] Therefore, the anion exchanges reported here are considered to be a solid-state phenomenon.

Experimental Section

Elemental analyses were recorded on a Perkin-Elmer 240C elemental analyzer at the Center of Materials Analysis, Nanjing University. ¹H NMR spectra were recorded a Bruker DRX500 NMR spectrometer. IR spectra

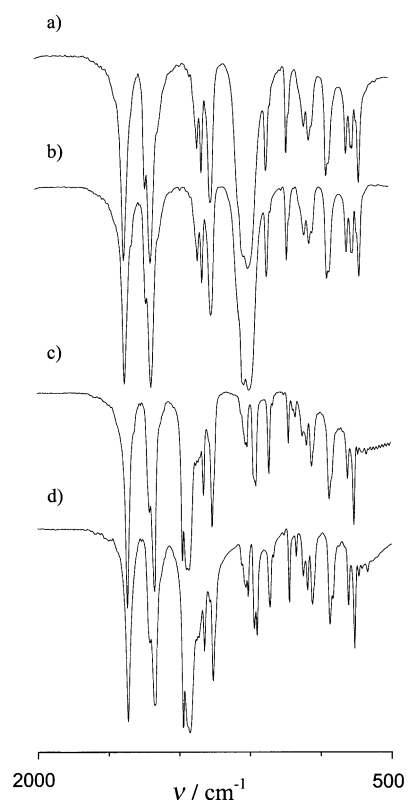


Figure 5. FT-IR spectra of a) complex **6** treated with aqueous solution of NaClO_4 , b) complex **5**, c) complex **6** treated with an aqueous solution of NaClO_4 and then with NaNO_3 , d) complex **6**.

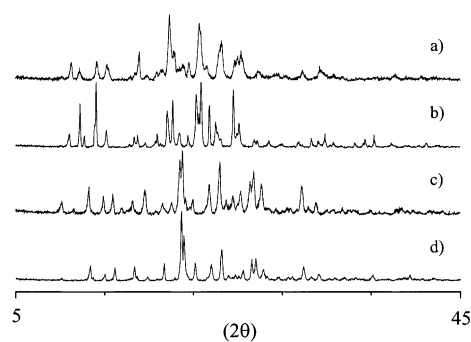


Figure 6. X-ray powder diffraction patterns of a) complex **6** treated with an aqueous solution of NaClO_4 ; b) complex **5**; c) complex **6** treated with an aqueous solution of NaClO_4 and then with NaNO_3 ; d) complex **6**.

were recorded on a Bruker Vector22 FT-IR spectrophotometer in KBr discs. Powder X-ray diffraction patterns were recorded on a Rigaku D/max-RA rotating anode X-ray diffractometer with graphite-monochromated $\text{Cu K}\alpha$ radiation (λ 1.542 Å) at room temperature. The concentration of manganese(II) ion was measured by atomic absorption spectroscopy on a Hitachi 180–80.

Safety note: Perchlorate salts of metal complexes with organic ligands are potentially explosive and should be handled with care.

Synthesis of ligand 3: 1,3,5-Tribromobenzene (2.52 g, 8.0 mmol), imidazole (3.26 g, 48.0 mmol), K_2CO_3 (4.42 g, 32.0 mmol), and $CuSO_4$ (0.05 g, 0.20 mmol) were mixed and heated at 180 °C for 12 h under a nitrogen atmosphere. The mixture was cooled to the room temperature, and was then washed with water. The residue was extracted with CH_2Cl_2 (5 × 30 mL). The organic layer was separated, dried over sodium sulfate, and evaporated to dryness to give the crude product **3**, which was recrystallized from water and ethanol. Yield: 67%; 1H NMR [$(CD_3)_2SO$]: δ = 8.86 (s, 3H), 8.35 (s, 3H), 8.27 (s, 3H), 7.49 ppm (s, 3H); elemental analysis calcd (%) for $C_{15}H_{12}N_6$: C 65.21, H 4.38, N 30.42; found C 65.37, H 4.48, N 30.39.

Synthesis of ligand 4: 3,5-Dibromotoluene was treated with *N*-bromosuccinimide to give 3,5-dibromobenzyl bromide, which was then treated with imidazole in DMSO to generate 1,3-dibromo-5-(imidazol-1-ylmethyl)benzene. Ligand **4** was prepared similarly to ligand **3** by the reaction of the imidazole with 1,3-dibromo-5-(imidazol-1-ylmethyl)benzene. Total yield: 29% (based on 3,5-dibromotoluene); 1H NMR [$(CD_3)_2SO$]: δ = 8.68 (s, 2H), 8.24 (s, 1H), 8.21 (s, 1H), 8.15 (s, 2H), 7.94 (s, 2H), 7.66 (s, 1H), 7.45 (s, 2H), 7.26 (s, 1H), 5.58 ppm (s, 2H); anal. calcd (%) for $C_{16}H_{14}N_6$: C 66.19, H 4.86, N 28.95; found C 66.11, H 4.77, N 29.02.

Synthesis of $[Mn(3)_2(H_2O)_2](ClO_4)_2 \cdot 2H_2O$ (5): This compound was prepared by a layering method: a buffer layer of methanol and water (2:1, 10 mL) was carefully layered over a solution of $Mn(ClO_4)_2 \cdot 6H_2O$ (36.2 mg, 0.1 mmol) in water (5 mL). Then a solution of **3** (27.6 mg, 0.1 mmol) in methanol was layered over the buffer layer. Single crystals appeared after several weeks. Yield: 57% (based on the ligand); elemental analysis calcd (%) for $C_{30}H_{32}Cl_2MnN_{12}O_{12}$: C 41.02, H 3.67, N 19.13; found C 41.20, H 3.55, N 19.14.

Synthesis of $[Mn(3)_2(H_2O)_2](NO_3)_2$ (6): The title complex was obtained similarly to compound **5** from $Mn(NO_3)_2 \cdot 6H_2O$ instead of $Mn(ClO_4)_2 \cdot 6H_2O$. Yield: 49%; elemental analysis calcd (%) for $C_{30}H_{28}MnN_{14}O_8$: C 46.94, H 3.68, N 25.55; found C 46.98, H 3.62, N 25.37.

Synthesis of $[Mn(3)_2(N_3)_2] \cdot 2H_2O$ (7): A buffer layer of a solution of NaN_3 (13.0 mg, 0.2 mmol) in methanol and water (2:1, 10 mL) was carefully layered over a solution of $Mn(CH_3COO)_2 \cdot 4H_2O$ (24.5 mg, 0.1 mmol) in water (5 mL). Then a solution of **3** (27.6 mg, 0.1 mmol) in methanol was layered over the buffer layer. Single crystals appeared after several weeks. Yield: 37% (based on the ligand); elemental analysis calcd (%) for $C_{30}H_{28}MnN_{18}O_2$: C 49.52, H 3.88, N 34.65; found C 49.58, H 3.91, N 34.11.

Synthesis of $[Cu(3)_2(H_2O)_2](ClO_4)_2$ (8): A mixture of $Cu(ClO_4)_2 \cdot 6H_2O$ (37.0 mg, 0.1 mmol), **3** (55.2 mg, 0.2 mmol), and H_2O (10 mL) was kept in a Teflon liner autoclave at 140 °C for 24 h. After the mixture had been cooled to room temperature, blue platelike crystals were collected. Yield: 42%; elemental analysis calcd (%) for $C_{30}H_{28}Cl_2CuN_{12}O_{10}$: C 42.34, H 3.32, N 19.75; found C 42.36, H 3.50, N 19.77.

Synthesis of $[Mn(4)_2(H_2O)(SO_4)] \cdot CH_3OH \cdot 5H_2O$ (9): $MnSO_4 \cdot H_2O$ (15.9 mg, 0.1 mmol) in water (5 mL) was added slowly with constant stirring to **4** (58 mg, 0.2 mmol) in methanol (20 mL) to give a clear solution. The reaction mixture was left to stand at room temperature for several days. Colorless crystals were obtained. Yield: 51%; elemental analysis calcd (%) for $C_{33}H_{44}MnN_{12}O_{11}S$: C 45.47, H 5.09, N 19.28; found C 45.52, H 5.11, N 19.24.

Synthesis of $[Mn(4)_2](ClO_4)_2$ (10): The compound was prepared similarly to compound **5** from ligand **4** instead of ligand **3**. Yield: 54%; elemental analysis calcd (%) for $C_{32}H_{28}Cl_2MnN_{12}O_8$: C 46.06, H 3.38, N 20.14; found C 46.19, H 3.58, N 20.11.

Reversible anion-exchange reactions: Well-ground powder of $[Mn(3)_2(H_2O)_2](NO_3)_2$ (**6**, 200.0 mg) was suspended in water (20 mL), then $NaClO_4$ (2.0 g) was added. The mixture was stirred for one day at room temperature, then filtered, washed with water several times, and dried to give a colourless powder. Elemental analysis calcd (%) for $[Mn(3)_2(H_2O)_2](ClO_4)_2 \cdot 2H_2O$: C 41.02, H 3.67, N 19.13; found C 41.14, H 3.56, N 19.04. The exchanged solid (200.0 mg) was suspended in water (20 mL), and $NaNO_3$ (2.0 g) was added. The mixture was stirred for one day at room temperature, then filtered, washed with water several times, and dried. Elemental analysis calcd (%) for $[Mn(3)_2(H_2O)_2](NO_3)_2$: C 46.94, H 3.67, N 25.55; found C 46.95, H 3.76, N 25.54.

Crystallography: The X-ray diffraction measurements for complexes **5** and **7** were performed on a SiemensP4 automatic four-circle diffractometer with graphite-monochromated MoK_{α} radiation ($\lambda = 0.71073 \text{ \AA}$) at room temperature. Intensity data were collected in the variable ω scan mode. The

structures were solved by direct methods using SHELX-97.^[18] Atoms Cl, O2, O3, O4, and O5 in complex **5** disordered into two positions and each position has site occupancy factors of 0.5. All non-hydrogen atoms were refined anisotropically, and the hydrogen atoms were generated geometrically. Calculations were performed on a PC-586 computer with the Siemens SHELXTL program package.^[19]

The intensity data for the complexes **6**, **8**, **9** and **10** were collected on a Rigaku/MSC Mercury CCD diffractometer with graphite-monochromated MoK_{α} radiation ($\lambda = 0.7107 \text{ \AA}$) at 173 K. The structures were solved by direct methods with SHELX-97^[18] and the non-hydrogen atoms were refined anisotropically by means of the full-matrix least-square method. The hydrogen atoms were generated geometrically. Atoms O6, O8, and O10 in complex **10** have two positions, each with site occupancy factors of 0.5. Details of the crystal parameters, data collection and refinements for complexes **5**–**10** are summarized in Table 1, and selected bond lengths and angles are given in Table 2.

CCDC-189832 (**5**), CCDC-189833 (**6**), CCDC-189834 (**7**), CCDC-189835 (**8**), CCDC-189836 (**9**), and CCDC-189837 (**10**) contain the supplementary crystallographic data for this paper. These data can be obtained free of charge via www.ccdc.cam.ac.uk/conts/retrieving.html (or from the Cambridge Crystallographic Data Centre, 12 Union Road, Cambridge CB2 1EZ, UK; fax: (+44) 1223-336033; or deposit@ccdc.cam.ac.uk).

Acknowledgement

The authors are grateful to the National Natural Science Foundation of China for financial support of this work.

- [1] a) P. N. W. Baxter, *Comprehensive Supramolecular Chemistry*, Vol. 9 (Ed.: J.-M. Lehn), Pergamon, Oxford, **1996**, Chap. 5; b) A. J. Blake, N. R. Champness, P. Hubberstey, W.-S. Li, M. A. Withersby, M. Schröder, *Coord. Chem. Rev.* **1999**, *183*, 117; c) P. J. Hagrman, D. Hagrman, J. Zubieta, *Angew. Chem.* **1999**, *111*, 2798; *Angew. Chem. Int. Ed.* **1999**, *38*, 2638.
- [2] a) H. O. Stumpf, L. Ouahab, Y. Pei, P. Bergerat, O. Kahn, *J. Am. Chem. Soc.* **1994**, *116*, 3866; b) B.-Q. Ma, S. Gao, G. Su, G.-X. Xu, *Angew. Chem.* **2001**, *113*, 448; *Angew. Chem. Int. Ed.* **2001**, *40*, 434; c) M. J. Zaworotko, *Chem. Commun.*, **2001**, 1.
- [3] a) M. Fujita, Y. J. Kwon, S. Washizu, K. Ogura, *J. Am. Chem. Soc.* **1994**, *116*, 1151; b) Y.-C. Liang, R. Cao, W.-P. Su, M. Hong, W.-J. Zhang, *Angew. Chem.* **2000**, *112*, 3442; *Angew. Chem. Int. Ed.* **2000**, *39*, 3304.
- [4] a) R. D. Schnebeck, E. Freisinger, B. Lippert, *Angew. Chem.* **1999**, *111*, 235; *Angew. Chem. Int. Ed.* **1999**, *38*, 168; b) O. M. Yaghi, G. Li, H. Li, *Nature* **1995**, *378*, 703; c) L. Carlucci, G. Ciani, D. M. Proserpio, A. Sironi, *J. Am. Chem. Soc.* **1995**, *117*, 12861.
- [5] a) Q. Wu, A. Hook, S. Wang, *Angew. Chem.* **2000**, *112*, 4094; *Angew. Chem. Int. Ed.* **2000**, *39*, 3933; b) S. F. Liu, Q. Wu, H. L. Schmider, H. Aziz, N. X. Hu, Z. Popovix, S. Wang, *J. Am. Chem. Soc.* **2000**, *122*, 3671; c) N. Tamoto, C. Adachi, K. Nagai, *Chem. Mater.* **1997**, *9*, 1077.
- [6] N. Takeda, K. Umemoto, K. Yamaguchi, M. Fujita, *Nature* **1999**, *398*, 794.
- [7] a) C. S. Hong, S. K. Son, Y. S. Lee, M. J. Jun, Y. Do, *Inorg. Chem.* **1999**, *38*, 5602; b) D. Sun, R. Cao, Y. Liang, Q. Shi, W. Su, M. Hong, *J. Chem. Soc. Dalton Trans.* **2001**, 2335.
- [8] a) M. Fujita, S.-Y. Yu, T. Kusukawa, H. Funaki, K. Ogura, K. Yamaguchi, *Angew. Chem.* **1998**, *110*, 2192; *Angew. Chem. Int. Ed.* **1998**, *37*, 2082; b) M. Fujita, N. Fujita, K. Ogura, K. Yamaguchi, *Nature* **1999**, *400*, 52; c) S. R. Batten, B. F. Hoskins, R. Robson, *Angew. Chem.* **1995**, *107*, 884; *Angew. Chem. Int. Ed. Engl.* **1995**, *34*, 820; d) S. R. Batten, B. F. Hoskins, R. Robson, *J. Am. Chem. Soc.* **1995**, *117*, 5385; e) D. M. L. Goodgame, D. A. Grachvogel, D. J. Williams, *Angew. Chem.* **1999**, *111*, 217; *Angew. Chem. Int. Ed.* **1999**, *38*, 153.
- [9] a) W. Y. Sun, J. Fan, T.-a. Okamura, J. Xie, K.-B. Yu, N. Ueyama, *Chem. Eur. J.* **2001**, *7*, 2557; b) J. Fan, W. Y. Sun, T.-a. Okamura, J. Xie, W.-X. Tang, N. Okamura, *New J. Chem.* **2002**, *26*, 199; c) H. K. Liu, W. Y. Sun, D. J. Ma, K. B. Yu, W.-X. Tang, *Chem. Commun.* **2000**, 591;

- d) H. K. Liu, W. Y. Sun, W.-X. Tang, T. Yamamoto, N. Ueyama, *Inorg. Chem.* **1999**, *38*, 6313.
- [10] J. S. Fleming, K. L. V. Mann, C.-A. Carraz, E. Psillakis, J. C. Jeffery, J. A. McCleverty, M. D. Ward, *Angew. Chem.* **1998**, *110*, 1315; *Angew. Chem. Int. Ed.* **1998**, *37*, 1279.
- [11] a) P. N. W. Baxter, J.-M. Lehn, G. Baum, D. Fenske, *Chem. Eur. J.* **1999**, *5*, 102; b) P. N. W. Baxter, J.-M. Lehn, B. O. Kneisel, G. Baum, D. Fenske, *Chem. Eur. J.* **1999**, *5*, 113; c) D. T. Tran, P. Y. Zavalij, S. R. J. Oliver, *J. Am. Chem. Soc.* **2002**, *124*, 3966.
- [12] a) O. M. Yaghi, H. Li, *J. Am. Chem. Soc.* **1995**, *117*, 10401; b) O. M. Yaghi, H. Li, C. Davis, D. Richardson, T. L. Groy, *Acc. Chem. Res.* **1998**, *31*, 474.
- [13] a) D. Braga, F. Grepioni, *Acc. Chem. Res.* **2000**, *33*, 601; b) J. Cai, C.-H. Chen, X.-L. Feng, C.-Z. Liao, X.-M. Chen, *J. Chem. Soc. Dalton Trans.* **2001**, 2370.
- [14] a) B. L. Fei, W. Y. Sun, Y. A. Zhang, K. B. Yu, W. X. Tang, *J. Chem. Soc. Dalton. Trans.* **2000**, 2345; b) L. Ballester, I. Baxter, P. C. M. Duncan, D. M. L. Goodgame, D. A. Grachvogel, D. J. Williams, *Polyhedron* **1998**, *17*, 3613.
- [15] a) G. B. Gardner, D. Venkataraman, J. S. Moore, S. Lee, *Nature* **1995**, *374*, 792; b) H. J. Cho, M. P. Suh, *J. Am. Chem. Soc.* **1998**, *120*, 10622.
- [16] a) D. W. Breck, *Zeolite Molecular Sieves, Structure, Chemistry, and Use*, Wiley, New York, **1974**; b) T. M. Reineke, M. Eddaoudi, M. Fehr, D. Kelley, O. M. Yaghi, *J. Am. Chem. Soc.* **1999**, *121*, 1651; c) R. Cao, D. Sun, Y. Liang, M. Hong, K. Tatsumi, Q. Shi, *Inorg. Chem.* **2002**, *41*, 2087.
- [17] A. N. Khlobystov, N. R. Champness, C. J. Roberts, S. J. B. Tendler, C. Thompson, M. Schröder, *CrystEngComm.*, **2002**, *4(71)*, 426.
- [18] a) G. M. Sheldrick, SHELX97, Program for Crystal Structure Determination, University of Göttingen, **1997**; b) G. M. Sheldrick, SHELX97, Program for Crystal Structure Refinement, University of Göttingen, **1997**.
- [19] a) XSCANS, Version 2.1, Siemens Analytical X-ray Instruments, Madison, WI, **1994**; b) SHELEXTL, Version 5.0, Siemens Industrial Automation, Analytical Instruments, Madison, WI, **1995**.

Received: July 29, 2002

Revised: March 17, 2003 [F4298]